

Magnetic properties of rare-earth antiferromagnets studied using a two-ion modelZ.-S. Liu,^{1,*} M. Diviš,² and V. Sechovský²¹*Faculty of Mathematics and Physics, Nanjing University of Information Science and Technology, Nanjing 210044, China*²*Department of Condensed Matter Physics, Faculty of Mathematics and Physics, Charles University, Ke Karlovu 5, 121 16 Prague 2, Czech Republic*

(Received 8 August 2008; revised manuscript received 13 October 2008; published 5 December 2008)

In this paper, a two-ion model for rare-earth antiferromagnets is proposed and employed to describe the magnetic behavior of $\text{HoNi}_2\text{B}_2\text{C}$ and DyFe_2Si_2 at low temperatures. The calculated temperature dependence of the susceptibilities and magnetizations along the hard and easy directions, respectively, shows very good agreement with experimental results.

DOI: [10.1103/PhysRevB.78.214409](https://doi.org/10.1103/PhysRevB.78.214409)

PACS number(s): 75.50.Ee, 75.10.Dg

I. INTRODUCTION

The $\text{RNi}_2\text{B}_2\text{C}$ compounds have attracted great research interest because of their interesting superconducting and magnetic properties.¹⁻⁷ In these materials, the superconducting transition temperature T_C is usually very close to the antiferromagnetic ordering temperature T_N . Consequently, comparable values of the magnetic and superconducting condensation energies yield strong interplay between the superconductivity and magnetic orderings, which was studied extensively by many authors.⁸⁻¹⁵

$\text{RNi}_2\text{B}_2\text{C}$ crystallizes in the tetragonal structure, in which the R - C layers alternate along the c axis with the Ni_2B_2 layers.¹⁶⁻¹⁸ Magnetic ordering in this system arises solely from the exchange interaction between the rare-earth ions bearing the localized $4f$ electron magnetic moments. No ordered magnetic moment has been detected on the Ni site.¹⁹

Among the members of the $\text{RNi}_2\text{B}_2\text{C}$ family, $\text{HoNi}_2\text{B}_2\text{C}$ exhibits the most interesting and complex superconducting properties. It begins to superconduct at about 8 K, then returns to the normal state at 5 K, and later re-enters the superconducting state again with further decreasing temperature.¹⁵ Obviously, these features are closely related to the magnetic phenomena in the vicinity of the magnetic ordering temperature.^{9,10} Below the ordering temperature of 8.5 K,¹⁹ the Ho moments in $\text{HoNi}_2\text{B}_2\text{C}$ order antiferromagnetically with two coexisting antiferromagnetic structures (a dominant one commensurate and a minor one incommensurate). However below 5 K where the superconductivity is re-entrant, only the commensurate antiferromagnetic structure exists.¹⁹ The Ho moments in each Ho- C layer order ferromagnetically, and the adjacent bilayers are coupled antiferromagnetically along the c axis. The ordered Ho moment was observed to be $8.62(6)\mu_B$ at a very low temperature by Skanthakumar *et al.*¹⁹

To describe the low-temperature metamagnetic phase diagram of $\text{HoNi}_2\text{B}_2\text{C}$, Amici *et al.*⁸ proposed a microscopic theory and obtained good agreement with experiments. They indicated that the complex behaviors of the system originate from the competition between the crystalline electric field and the Ruderman-Kittel-Kasuya-Yosida (RKKY) interaction, no essential influence of superconductivity has been involved in the magnetic process of this material.

On the other hand, in order to study the magnetic properties of $\text{RNi}_2\text{B}_2\text{C}$ system quantitatively, Gasser *et al.*²⁰ con-

ducted inelastic neutron scattering to determine the crystal-field (CF) parameters (CFPs) for the compounds with $R = \text{Ho}$, Er , and Tm . These parameters were then used to estimate the CFPs of other members of the family with extrapolation approach.²¹ Using the CFPs such obtained, they further calculated the susceptibilities and magnetic specific heats of $\text{HoNi}_2\text{B}_2\text{C}$, $\text{ErNi}_2\text{B}_2\text{C}$, and $\text{TmNi}_2\text{B}_2\text{C}$ to make comparison with experimental results.²⁰ Indeed, their calculated susceptibilities are well consistent with the measured data *above* the magnetic transition temperatures. However below T_N , their theoretical susceptibility curves in external magnetic fields along the easy axis tend to extremely large values, showing evident deviations from the experimental results.

As observed in the susceptibility curve of $\text{HoNi}_2\text{B}_2\text{C}$ measured in an external magnetic field within the easy ab plane,^{20,22} the susceptibility increases gradually from zero well below the Néel temperature; it reaches the maximum at $T_N = 5.7$ K,^{22,23} then attenuates continuously with further increasing temperature. This result indicates that at temperatures well below T_N , the material remains antiferromagnetic even in a weak external magnetic field; as the temperature rises, the magnetic moments antiparallel to the external magnetic field are gradually rotated by the external force to the field direction.

Generally speaking, the above magnetic process actually occurs in all rare-earth antiferromagnets at low temperatures, as, for example, observed in DyFe_2Si_2 . This material crystallizes in the body-centered tetragonal crystal structure of the ThCr_2Si_2 type, in which the Dy, Fe, or Si layers are stacked alternatively along the c axis.²⁴ Powder neutron-diffraction experiment has observed that the Dy moments are sine modulated with the propagation vector $k = (0.335, 0, 0.135)$ below Néel temperature $T_N (= 3.9 \text{ K})$.²⁵ No magnetic moment was detected on the Fe sites as confirmed by ⁵⁷Fe and ¹⁶¹Dy Mössbauer spectroscopy.²⁶⁻²⁸

Recently, Mihalik *et al.*²⁹ measured the magnetization, ac susceptibility, and specific heat on a single-crystal sample of DyFe_2Si_2 in external magnetic fields. Using the CFPs determined by fitting the experimental susceptibility, they calculate the magnetizations of the material in external magnetic fields up to 14 T along the c axis and in the basal plane at $T = 2$ and 20 K, respectively.

Inspecting the magnetization curve measured in an external field exerted along the c direction at $T = 2$ K, the magne-

tization increases gradually from zero, passing a metamagnetic transition (MT) around 1 T, and becomes almost saturated in a higher field. This behavior also suggests that in a weak external magnetic field below the MT the material be still antiferromagnetic; only when the magnetic field is sufficiently strong, the moments which are antiparallel to the magnetic field can be totally rotated by the magnetic field to its direction.

To generate the magnetic ordering of a rare-earth magnet below the magnetic transition temperature theoretically, the RKKY exchange interaction between each pair of the neighboring magnetic ions must be considered. Especially, to mimic the magnetic process of an antiferromagnet below T_N just described above, the single-ion model is obviously inadequate. To solve the problem, we developed a two-ion model as underlined below and used it to the two systems. For DyFe_2Si_2 , we have derived analytic formulas for the magnetization of the material with the lowest CF states; whereas for $\text{HoNi}_2\text{B}_2\text{C}$, we have only conducted numerical computations.

II. TWO-ION MODEL

In this model, the rare-earth ions A and B are all subject to the interaction of the crystal electric field (CEF) formed by the surrounding electric charges; the A ion interacts with another A ion and a B ion nearby through RKKY exchange interaction with coupling constants λ_{11} and λ_{12} , respectively; the B ion with another B ion and the A ion nearby with coupling constants λ_{22} and λ_{21} , respectively. That is, the A and B ions form two sublattices, which are coupled together by λ_{12} and λ_{21} . Hence, the Hamiltonians of the system with two sublattices are expressed with

$$\mathcal{H}^{(A)} = \mathcal{H}_{\text{CF}} - \lambda_{11} \mathbf{J} \cdot \langle \mathbf{J}^{(A)} \rangle - \lambda_{12} \mathbf{J} \cdot \langle \mathbf{J}^{(B)} \rangle - \mu_B g_J \mathbf{B} \cdot \mathbf{J},$$

$$\mathcal{H}^{(B)} = \mathcal{H}_{\text{CF}} - \lambda_{22} \mathbf{J} \cdot \langle \mathbf{J}^{(B)} \rangle - \lambda_{21} \mathbf{J} \cdot \langle \mathbf{J}^{(A)} \rangle - \mu_B g_J \mathbf{B} \cdot \mathbf{J}. \quad (1)$$

Actually, the present model can be derived from that previously proposed by Amici⁸ if we only consider the RKKY exchange coupling among the nearest rare-earth magnetic ions. For convenience, we chose $\lambda_{11} = \lambda_{22} = \lambda_1$ and $\lambda_{12} = \lambda_{21} = \lambda_2$. For $\text{HoNi}_2\text{B}_2\text{C}$ they were found to be $\lambda_1 = 0.08$ K and $\lambda_2 = -0.10$ K, respectively, by fitting its measured susceptibility curves and T_N .^{22,23} In Amici's paper,⁸ the two coupling parameters λ_1 and λ_2 were denoted as \mathcal{J}_0 and \mathcal{J}_1 , respectively, and their calculations gave $\mathcal{J}_0 = 4.8 \times 10^{-3}$ meV = 0.06 K and $\mathcal{J}_1 = -8 \times 10^{-3}$ meV = -0.09 K, which are very close to those we presented above. Obviously, the positive value of λ_1 suggests the Ho ions in the same Ho-C layer be coupled ferromagnetically; the negative value of λ_2 means that the ions in the adjacent layers coupled antiferromagnetically.

III. APPLICATION TO $\text{HoNi}_2\text{B}_2\text{C}$

Even though the Hamiltonians of the two ions are coupled together through $\langle J_A \rangle$ and $\langle J_B \rangle$, they were actually diagonalized separately to calculate $\langle J_A \rangle$ and $\langle J_B \rangle$, respectively, in each loop during iterations. Using the crystal-field param-

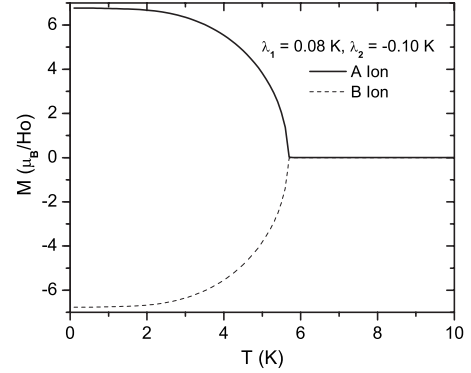


FIG. 1. The calculated magnetizations of the A and B sublattices of $\text{HoNi}_2\text{B}_2\text{C}$ plotted as functions of temperature in the absence of external magnetic field. Here the exchange constants $\lambda_1 = 0.08$ K and $\lambda_2 = -0.10$ K are used.

eters $A_2^0 = -14.5$ meV, $A_4^0 = 2.3$ meV, $A_4^4 = -71.4$ meV, $A_6^0 = -0.42$ meV, and $A_6^4 = 11.7$ meV for $\text{HoNi}_2\text{B}_2\text{C}$, which were determined by Gasser *et al.*²⁰ in a neutron-scattering experiment, we first calculated the spontaneous magnetizations of the two sorts of Ho ions at low temperatures as depicted in Fig. 1. The material exhibits strong anisotropy below T_N ; its magnetic moments only order spontaneously in the ab plane in the absence of external field. Our calculated magnetization M_A of the A ion is always positive, but M_B of the B ion is always negative below the Néel temperature, manifesting the antiferromagnetic nature of the rare-earth magnet. At $T = 0.1$ K, the spontaneous magnetization is found to be $6.77 \mu_B$ per Ho ion, which is considerably lower than the experimentally observed value of $8.62(6) \mu_B$ detected by Skanthakumar *et al.*,¹⁹ demonstrating that both the magnetic and superconducting states are very sensitive functions of the sample composition.^{30,31} Actually, the different Néel temperatures, from 5.1 to 9.8 K, were reported for $\text{HoNi}_2\text{B}_2\text{C}$ by several research groups.^{19,22,32} Obviously, the magnetic moment of a sample with $T_N = 8.5$ K (Ref. 19) should be larger than a sample with $T_N = 5.7$ K (Refs. 22 and 23) at the same temperature.

With the CFPs and the exchange coupling constants given above, we further calculated the susceptibilities in external magnetic fields of 0.01 T exerted along the a and c axes, respectively; such obtained results are depicted as functions of temperature in Fig. 2 in comparison with the experimental data.²² The theoretical curves along the two directions show very good agreement with the experimental ones. Especially, our theoretical curve along the easy a axis starts to grow from almost zero at very low temperatures, increases gradually with the rising temperature, exhibits a sharp peak at T_N , and then decays afterwards as observed in the experiment.

To understand the complicated magnetic process involved at low temperatures for the antiferromagnet, we also calculated the susceptibilities of the two sublattices separately, and then the overall values, that is, the sum of the two sublattices, in an external magnetic field of 0.01 T applied along the easy a direction. The theoretical results are displayed as the functions of temperature in Fig. 3. As shown in the figure, the magnetic moment of the A ion always orders along the a axis, that is, parallel to the external magnetic field; the

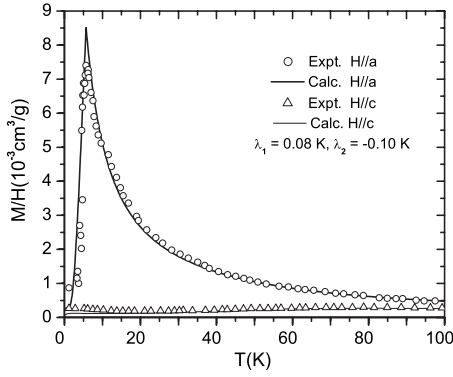


FIG. 2. The calculated susceptibilities of $\text{HoNi}_2\text{B}_2\text{C}$ plotted as the functions of temperature with external magnetic fields applied in the a and c directions, respectively, in comparison with experimental results (Ref. 22). Here $\lambda_1=0.08$ K and $\lambda_2=-0.10$ K are used.

susceptibility of the A sublattice decays gradually from $597.81 \times 10^{-3} \text{ cm}^3/\text{g}$ at $T=0.1$ K, an extremely larger value than the experimental value, to $4.46 \times 10^{-3} \text{ cm}^3/\text{g}$ while the temperature is rising to $T=5.7$ K. On the other hand, the magnetic moment of ion B orders along the negative a axis, that is, antiparallel to the external field direction below T_N ; the susceptibility of the B sublattice starts from $-597.55 \times 10^{-3} \text{ cm}^3/\text{g}$ at $T=0.1$ K, which slightly differs from that of the A sublattice at the same temperature, and then attenuates continuously due to the disturbance of increasing temperature; it jumps suddenly from a negative value $-116.23 \times 10^{-3} \text{ cm}^3/\text{g}$ at $T=5.6$ K to $4.05 \times 10^{-3} \text{ cm}^3/\text{g}$ at $T=5.7$ K and then decreases slowly. The relatively very large opposite moments of the two sublattices offset at low temperatures. As a result, the overall susceptibility of the antiferromagnet exhibits much smaller and reasonable magnitude below T_N , it increases gradually from zero with the rising temperature, reaches a maximum at T_N , and then

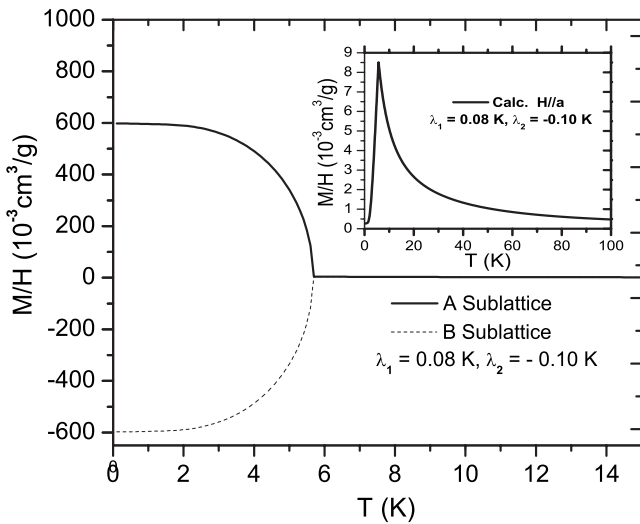


FIG. 3. The calculated susceptibilities of A and B sublattices, as well as their sum values of $\text{HoNi}_2\text{B}_2\text{C}$ plotted as the functions of temperature with the external magnetic field applied in the a direction. Here $\lambda_1=0.08$ K and $\lambda_2=-0.10$ K are used.

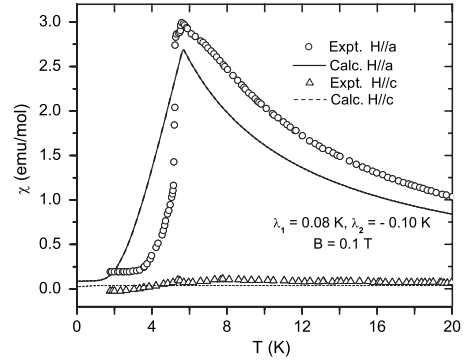


FIG. 4. The calculated susceptibility curves of $\text{HoNi}_2\text{B}_2\text{C}$ at low temperatures in comparison with experimental results (Ref. 23), where the external magnetic fields, $B=0.1$ T, are applied in the a and c directions, respectively, $\lambda_1=0.08$ K and $\lambda_2=-0.10$ K are used.

abates afterwards, as shown in Fig. 2 and the inset of Fig. 3. However, when the external magnetic field of the same strength is exerted in the hard c direction, the theoretical susceptibilities for the two sublattices were found to be same in the whole temperature range; thus the overall susceptibility is simply equal to two times of each sublattice as displayed in Fig. 2, meaning that the A and B sublattices respond to the external magnetic field with same sensitivity.

To further test our two-ion model and demonstrate its utility, we also calculated the susceptibilities of the compound in an external magnetic field with strength of 0.1 T applied in the a and c directions, respectively. The theoretical results are displayed in Fig. 4 in comparison with the experimental data obtained by Ribeiro *et al.*²³ Our calculated curves along the two directions exhibit the tendency and magnitude very similar to the experimental ones. The small deviation in the a direction might be attributed to the different samples used in experiments. As indicated by Lynn and Schmidt *et al.*,^{30,31} the magnetic and superconducting properties of $\text{HoNi}_2\text{B}_2\text{C}$ are very sensitive to the sample composition.^{30,31}

IV. APPLICATION TO DyFe_2Si_2

With the crystal-field parameters $A_2^0=329$ K, $A_4^0=-3$ K, $A_4^4=-130$ K, $A_6^0=19$ K, and $A_6^4=160$ K determined by Mihalik *et al.*²⁹ for the compound, the ground CF level is found to be a doublet,

$$|\varphi_{1,2}^{(0)}\rangle = a \left| \pm \frac{15}{2} \right\rangle + b \left| \pm \frac{7}{2} \right\rangle + c \left| \mp \frac{1}{2} \right\rangle + d \left| \mp \frac{9}{2} \right\rangle, \quad (2)$$

where $a=0.99646$, $b=-0.08409$, $c=0.00109$, and $d=-0.0007$; the first excited CF level is also a doublet,

$$|\varphi_{3,4}^{(0)}\rangle = r \left| \pm \frac{13}{2} \right\rangle + s \left| \pm \frac{5}{2} \right\rangle + t \left| \mp \frac{3}{2} \right\rangle + u \left| \mp \frac{11}{2} \right\rangle, \quad (3)$$

with $r=0.99417$, $s=-0.10781$, $t=-0.00108$, and $u=0.00028$ situated at $\epsilon_1^{(0)}=33.019$ K above the ground CF level; and the second excited CF level is a doublet as well,

$$|\varphi_{5,6}^{(0)}\rangle = 0.990\,84 \left| \pm \frac{11}{2} \right\rangle - 0.135\,05 \left| \pm \frac{3}{2} \right\rangle - 0.001\,97 \left| \mp \frac{5}{2} \right\rangle - 0.000\,64 \left| \mp \frac{13}{2} \right\rangle, \quad (4)$$

with eigenenergy $\epsilon_2^{(0)} = 127.853$ K.

Carefully inspecting the CF states, we believe the magnetic process of the material in the easy c direction at low temperatures is mainly governed by the two lowest CF states. Taking these two states $|\varphi_{1,2}^{(0)}\rangle$ as bases for the two-ion Hamiltonians, it is easy to find that the wave functions of the A and B ions remain unchanged, that is, $|\psi_{1,2}^{(A,B)}\rangle = |\varphi_{1,2}^{(0)}\rangle$, respectively, even under the interaction of the molecular field; however the two original CF states are shifted to $\epsilon_{1,2}^{(A,B)} = \pm \xi \mathcal{F}_{A,B}(T)$, respectively, where $\xi = 7.5a^2 + 3.5b^2 - 0.5c^2 - 4.5d^2 = 7.471\,74$, $\mathcal{F}_A(T) = \lambda_1 \langle J_A \rangle + \lambda_2 \langle J_B \rangle + \mu_B g_J B$, and $\mathcal{F}_B(T) = \lambda_1 \langle J_B \rangle + \lambda_2 \langle J_A \rangle + \mu_B g_J B$. Here the RKKY exchange constants were found to be $\lambda_1 = 0.01$ K and $\lambda_2 = -0.06$ K, respectively, by fitting the measured magnetization curves and the T_N of the material. Through many steps of algebraic manipulations with quantum theory, we derived a formula for the thermally averaged total angular momentum,

$$\langle J_A \rangle = \xi \tanh\left(\frac{\xi \mathcal{F}_A(T)}{k_B T}\right), \quad (5)$$

for the A ion. Following the same steps, we have also got

$$\langle J_B \rangle = \xi \tanh\left(\frac{\xi \mathcal{F}_B(T)}{k_B T}\right) \quad (6)$$

for the B ion.

Having Eqs. (5) and (6) we are able to estimate T_N theoretically. In zero external field, when $T \rightarrow T_N$, $\langle J_A \rangle = -\langle J_B \rangle \rightarrow 0$, thus $\mathcal{F}_A(T) = \mathcal{F}_B(T) \rightarrow 0$ as well. Using $\tanh(x) \approx x - \frac{x^3}{3}$ as $|x| \ll 1$ and by omitting the last term, we then have

$$T_N = \frac{\xi^2(\lambda_1 - \lambda_2)}{k_B}. \quad (7)$$

Substituting the values of ξ and $(\lambda_1 - \lambda_2)$ into this formula, we obtain the Néel temperature $T_N = 3.908$ K precisely for the antiferromagnet. With Eqs. (5) and (6), we can also determine the initial values of $M_c^{(A)}$ and $M_c^{(B)}$ theoretically. At $T=0$, the magnetic process is solely governed by the new ground state. Thus the magnetization

$$\langle M_c^{(A)} \rangle = -\langle M_c^{(B)} \rangle = \mu_B g_J \langle \psi_2^{(A)} | J_z | \psi_2^{(A)} \rangle = \xi g_J \mu_B = 9.962 \mu_B, \quad (8)$$

which is also the exact value we obtained numerically.

Varying the external magnetic field B exerted in the c direction from zero to 8 T, we calculated the magnetization of the material at $T=2$ K with Eq. (5), Eq. (6), and the expressions of $\mathcal{F}_{A,B}(T)$, as shown in Fig. 5 in comparison with experimental results. To understand the magnetic process involved, we also display our calculated magnetization curves of the two ions and their averaged value as the functions of the external field in the inset of the figure. The moment of the A ion always orders in the c direction; it drops

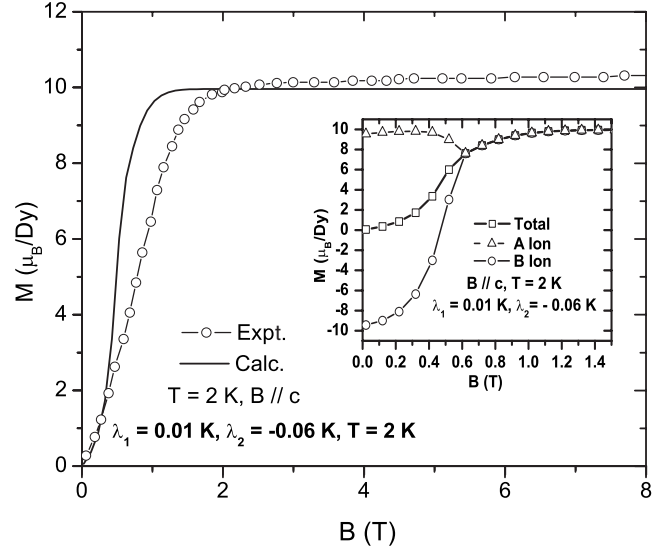


FIG. 5. The magnetization curves of the two ions and their average obtained with Eqs. (5) and (6) are plotted for DyFe_2Si_2 as the functions of the external magnetic field up to 8 T along the c direction at $T=2$ K in comparison with the experimental results. Here $\lambda_1=0.01$ K and $\lambda_2=-0.06$ K are used.

first from $9.543\mu_B$ to $7.618\mu_B$ as the field approaches from approximately 0 to 0.62 T due to its coupling with the B ion, it then increases gradually and becomes saturated above 2.2 T. On the other hand, when the external field is weaker than 0.5 T, the magnetic moment of the ion B orders in the opposite c direction, but its value increases continuously, suggesting that the moment be gradually rotated to the c direction by the external field. Afterwards, it still keeps increasing and becomes identical with that of the A ion above 0.6 T. Consequently, the averaged value of the two moments shows continuous increment from zero with the increasing field and reaches saturation above 2 T as shown in the figure, showing good agreement with the experimental curve.

To study the magnetization process of the crystalline along the hard a direction, we also took the two lowest CF states as bases to perform formulation as just done in this section. Now the two new magnetic states of the A ion are shifted to $\epsilon_{1,2}^{(A)} = \pm \eta \mathcal{F}_A(T)$, respectively, where $\eta = 4(c^2 + \sqrt{3}bd)$; they are found to be the mixtures of the two original CF states. Following the similar steps as done above, we finally arrive at

$$\langle J_A \rangle = \frac{2\eta}{z_A} \left[\alpha_1^{(A)} \beta_1^{(A)} \exp\left(-\frac{\epsilon_1^{(A)}}{k_B T}\right) + \alpha_2^{(A)} \beta_2^{(A)} \exp\left(-\frac{\epsilon_2^{(A)}}{k_B T}\right) \right], \quad (9)$$

for the A ion. Here the partition function,

$$z_A = \exp\left(-\frac{\epsilon_1^{(A)}}{k_B T}\right) + \exp\left(-\frac{\epsilon_2^{(A)}}{k_B T}\right), \quad (10)$$

where $\alpha_{1,2}^{(A)}$ and $\beta_{1,2}^{(A)}$ are the expanding coefficients of the new wave functions. These formulas hold true for the B ion if the superscripts A 's are replaced by B 's. With these formulas, we are able to investigate why the a axis is the hard direction. In

zero field, the two magnetic ions order in the opposite directions spontaneously below T_N , thus $\langle J_B \rangle = -\langle J_A \rangle$. Let us assume $\langle J_A \rangle > 0$. In this case, the eigenenergies of the two new states $\varepsilon_{1,2}^{(A)} = \pm \eta(\mathcal{J}_1 - \mathcal{J}_2)\langle J_A \rangle$, and $\varepsilon_2^{(A)} = -\eta(\mathcal{J}_1 - \mathcal{J}_2)\langle J_A \rangle < \varepsilon_1^{(A)}$ is the eigenvalue of the new ground state,

$$|\psi_g\rangle = \frac{1}{\sqrt{2}}(|\varphi_1^{(0)}\rangle - |\varphi_2^{(0)}\rangle). \quad (11)$$

Only this new state participates in magnetic ordering at $T=0$ and gives $\langle J_A \rangle = -\eta$, which is negative and contradictory to the original assumption, suggesting that no spontaneous magnetic ordering occurs in the a direction if only the lowest CF level is considered.

However, if the formulas just derived are used to calculate the magnetization in the a direction, no appreciable magnetic moment can be obtained even in a strong external magnetic field of 14 T. Based on the established theory,^{33,34} the states in the first and second excited CF levels also participate in the magnetic ordering since there exist nonzero matrix elements of J_+ and J_- between the three lowest levels. Therefore, when the three lowest CF levels are taken as bases to calculate the magnetization numerically, the agreement with the experimental results is considerably improved as shown in Fig. 6. Surprisingly, if all CF levels of the lowest J multiplet are included in numerical calculations, the magnetization remains almost unchanged in comparison with the one just obtained, as shown in the inset. Thus we conclude that $M_a(T)$ of DyFe_2Si_2 is governed by the lowest three CF levels. The deviation from the experimental above 9 T might be caused by the change in magnetic structure²⁹ or the quadrupolar interaction and magnetoelastic effect, which are usually induced by a strong magnetic field in compounds containing heavy rare-earth elements.³⁵

V. CONCLUSIONS AND DISCUSSIONS

$\text{HoNi}_2\text{B}_2\text{C}$ and DyFe_2Si_2 are different materials; so they have distinct physical properties. However, as antiferromagnets, they exhibit very similar features. At low temperatures, the two sorts of magnetic moments in each magnet align in the opposite directions even in a weak external magnetic field; the susceptibilities of the two sublattices are usually of very large magnitudes; however they mutually offset so that their sum values, which are usually observed in experiments, show much weaker magnitudes. As a result, the overall susceptibility in the easy direction increases gradually from al-

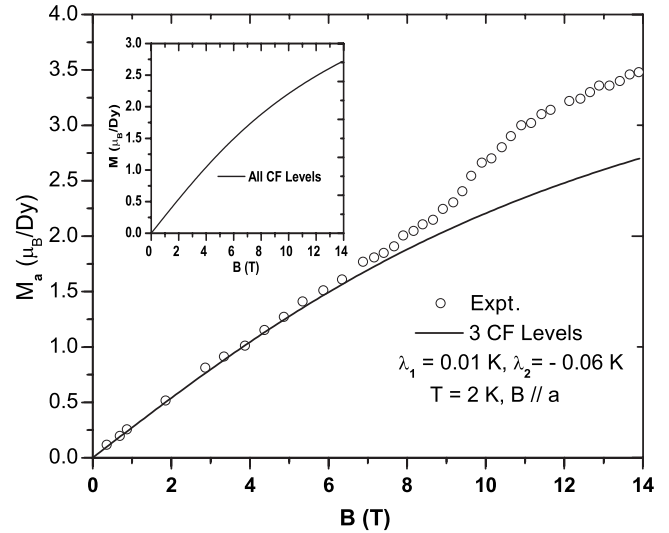


FIG. 6. The magnetization curves of DyFe_2Si_2 , obtained with the lowest three and all CF levels of the lowest J multiplet numerically, are plotted as the functions of the external magnetic fields applied in the a direction at $T=2$ K in comparison with experimental results. Here $\lambda_1=0.01$ K and $\lambda_2=-0.06$ K are used.

most zero at very low temperatures to a maximum at T_N as shown in Figs. 2 and 3. The two-ion model proposed here well mimics such magnetic process; therefore it has produced nice agreement with experiments. Of course, to describe the real magnetic process of rare-earth antiferromagnets with more complicated magnetic structures, a many-ion model is required, but more RKKY exchange constants are involved and needed to be determined. Consequently, the computations become tedious and very often impossible. In contrast, with this simplified two-ion model we are able to compute the susceptibilities and magnetic moments of the two sorts of sublattices and of course their overall values, which are usually measured directly in experiments, and to describe and understand the magnetic process of rare-earth antiferromagnets in order to study their magnetic properties quantitatively.

ACKNOWLEDGMENTS

Z.-S.L. was supported by Natural Science Foundation of Jiangsu Province, China under Grant No. BK2008438. The work of M.D. and V.S. is a part of the research plan under Grant No. MSM 0021620834 that was financed by the Ministry of Education of the Czech republic.

*liuzhs@yahoo.com.cn

¹M. B. Maple, *Physica B* **215**, 110 (1995).

²B. K. Cho, P. C. Canfield, and D. C. Johnston, *Phys. Rev. B* **52**, R3844 (1995).

³P. Dervenagas, J. Zarestky, C. Stassis, A. I. Goldman, P. C. Canfield, and B. K. Cho, *Physica B* **212**, 1 (1995).

⁴Q. Huang, A. Santoro, T. E. Grigereit, J. W. Lynn, R. J. Cava, J. J. Krajewski, and W. F. Peck, Jr., *Phys. Rev. B* **51**, 3701 (1995).

⁵S. K. Sinha, J. W. Lynn, T. E. Grigereit, Z. Hossain, L. C. Gupta, R. Nagarajan, and C. Godart, *Phys. Rev. B* **51**, 681 (1995).

⁶J. Zarestky, C. Stassis, A. I. Goldman, P. C. Canfield, P. Dervenagas, B. K. Cho, and D. C. Johnston, *Phys. Rev. B* **51**, 678 (1995).

⁷M. Kuznietz and H. Takeya, *Physica B* **281–282**, 1004 (2000).

⁸A. Amici and P. Thalmeier, *Phys. Rev. B* **57**, 10684 (1998).

⁹T. E. Grigereit, J. W. Lynn, Q. Huang, A. Santoro, R. J. Cava, J.

- J. Krajewski, and W. F. Peck, *Phys. Rev. Lett.* **73**, 2756 (1994).
- ¹⁰A. I. Goldman, C. Stassis, P. C. Canfield, J. Zarestky, P. Dervenagas, B. K. Cho, D. C. Johnston, and B. Sternlieb, *Phys. Rev. B* **50**, 9668 (1994).
- ¹¹P. Dervenagas, J. Zarestky, C. Stassis, A. I. Goldman, P. C. Canfield, and B. K. Cho, *Phys. Rev. B* **53**, 8506 (1996).
- ¹²L. J. Chang, C. V. Tomy, D. McK. Paul, and C. Ritter, *Phys. Rev. B* **54**, 9031 (1996).
- ¹³J. W. Lynn, S. Skanthakumar, Q. Huang, S. K. Sinha, Z. Hossain, L. C. Gupta, R. Nagarajan, and C. Godart, *Phys. Rev. B* **55**, 6584 (1997).
- ¹⁴A. Kreyssig, M. Lowenhaupt, K.-H. Müller, G. Fuchs, A. Handstein, and C. Ritter, *Physica B* **234–236**, 737 (1997).
- ¹⁵H. Eisaki, H. Takagi, R. J. Cava, B. Batlogg, J. J. Krajewski, W. F. Peck, K. Mizuhashi, J. O. Lee, and S. Uchida, *Phys. Rev. B* **50**, 647 (1994).
- ¹⁶T. Siegrist, H. W. Zandbergen, R. J. Cava, J. J. Krajewski, and W. F. Peck, Jr, *Nature (London)* **367**, 254 (1994).
- ¹⁷Q. Huang, J. W. Lynn, A. Santoro, B. C. Chakoumakos, R. J. Cava, J. J. Krajewski, and J. W. F. Peck, *Physica C* **271**, 311 (1996).
- ¹⁸L. J. Chang, C. V. Tomy, D. McK. Paul, N. H. Andersen, and M. Yethiraj, *J. Phys.: Condens. Matter* **8**, 2119 (1996).
- ¹⁹S. Skanthakumar and J. W. Lynn, *Physica B* **259–261**, 576 (1999).
- ²⁰U. Gasser, P. Allenspach, F. Fauth, W. Henggeler, J. Mesot, and A. Furrer, *Z. Phys. B* **101**, 345 (1996).
- ²¹U. Gasser, P. Allenspach, J. Mesot, and A. Furrer, *Physica C* **282–287**, 1327 (1997).
- ²²B. K. Cho, *Physica C* **298**, 305 (1998).
- ²³R. A. Ribeiro, S. L. Bud'ko, and P. C. Canfield, *J. Magn. Magn. Mater.* **267**, 216 (2003).
- ²⁴D. Rossi, R. Marazza, and R. Ferro, *J. Less-Common Met.* **58**, 203 (1978).
- ²⁵F. Bourée-Vignerot, M. Pinot, M. Golab, A. Szytuła, and A. Oleś, *J. Magn. Magn. Mater.* **86**, 383 (1990).
- ²⁶J. J. Bara, H. U. Hryniewicz, A. Miłoś, and A. Szytuła, *J. Less-Common Met.* **161**, 185 (1990).
- ²⁷P. Vulliet, K. Tomala, B. Malaman, G. Venturini, and J. P. Sanchez, *J. Magn. Magn. Mater.* **119**, 301 (1993).
- ²⁸D. R. Noakes, A. M. Umarji, and G. K. Shenoy, *J. Magn. Magn. Mater.* **39**, 309 (1983).
- ²⁹M. Mihalik, P. Svoboda, J. Ruzs, M. Diviš, and V. Sechovský, *Physica B* **367**, 19 (2005).
- ³⁰J. W. Lynn, Q. Huang, S. K. Sinha, Z. Hossain, L. C. Gupta, R. Nagarajan, and C. Godart, *Physica B* **223–224**, 66 (1996).
- ³¹H. Schmidt, M. Müller, and H. F. Braun, *Physica C* **235–240**, 779 (1994).
- ³²W. C. Lee, *Physica* **399**, 116 (2007).
- ³³Z.-S. Liu and S.-L. Guo, *Phys. Lett. A* **314**, 491 (2003).
- ³⁴Z.-S. Liu and S.-L. Guo, *Phys. Lett. A* **314**, 244 (2003).
- ³⁵V. M. T. S. Barthem, D. Gignoux, A. Näit-Saada, D. Schmitt, and G. Creuzet, *Phys. Rev. B* **37**, 1733 (1988).